

Color Breaking Baryogenesis

Michael J. Ramsey-Musolf,^{1,2,*} Graham White,^{3,4,†} and Peter Winslow^{1,‡}

¹*Physics Department, University of Massachusetts Amherst, Amherst, MA 01003, USA*

²*Kellogg Radiation Laboratory, California Institute of Technology, Pasadena, CA 91125, USA*

³*ARC Centre of Excellence for Particle Physics, Monash University, Victoria 3800, Australia*

⁴*TRIUMF, 4004 Wesbrook Mall, Vancouver, British Columbia V6T 2A3, Canada*

We propose a scenario that generates the observed baryon asymmetry of the Universe through a multi-step phase transition in which $SU(3)$ color symmetry is first broken and then restored. A spontaneous violation of $B - L$ conservation leads to a contribution to the baryon asymmetry that becomes negligible in the final phase. The baryon asymmetry is therefore produced exclusively through the electroweak mechanism in the intermediate phase. We illustrate this scenario with a simple model that reproduces the observed baryon asymmetry. We discuss how future electric dipole moment and collider searches may probe this scenario, though future EDM searches would require an improved sensitivity of several orders of magnitude.

I. INTRODUCTION

The origin of the cosmic matter-antimatter asymmetry remains one of the outstanding open questions at the interface of cosmology with particle and nuclear physics. The Planck experiment determines that the baryon asymmetry of the Universe (BAU) is [1]

$$\frac{n_B}{s} \equiv Y_B = (8.59 \pm 0.11) \times 10^{-11} \quad (1)$$

where n_B (s) is the baryon number (entropy) density. To dynamically generate the BAU one must fulfil three Sakharov conditions[2]: baryon number violation, C and CP violation, and a departure from equilibrium. The Standard Model (SM) cannot explain the matter-antimatter asymmetry as it fails to provide sufficient CP violation [3–5] and the required out-of-equilibrium conditions[6–9]. As such many beyond SM scenarios have arisen to accommodate this need.

For many years, electroweak baryogenesis (EWBG) has been one of the most attractive scenarios for explaining the BAU [10–12]. The main reason for this interest has been its testable nature due to its strong connection with the weak scale. However, successful electroweak baryogenesis requires new bosonic states with masses near the weak scale and significant couplings to the Higgs boson in order to generate a strongly first-order electroweak phase transition (EWPT). One of the most widely-considered possibilities, the minimal supersymmetric Standard Model (MSSM) with relatively light top squarks, appears to be in considerable tension with LHC data *e.g.*, see [13, 14] (however, see also [15]). In this context, it is worth asking if there are well motivated and testable modifications to the EWBG paradigm.

The rich landscape of phase structures in condensed matter systems suggests that the thermal history of sym-

metries in the Universe might be more exotic than the conventional scenario involving a single instance of electroweak symmetry-breaking at a temperature $T_{EW} \sim 100$ GeV. This possibility has been suggested in Weinberg’s analysis of gauge symmetries at finite temperature [16], and subsequently followed up by several authors[17–26]. As observed in Ref. [16], for example, Rochelle salt has the remarkable property first undergoing a symmetry-breaking transition as the temperature is lowered, followed by a symmetry-restoring transition at lower temperature[27]. This raises the fascinating possibility that a similar phenomenon may occur in gauge theories[16].

In light of this possibility and the constraints on the EWBG paradigm, we consider a multi-step phase transition beginning with a symmetric universe at high temperature, followed by the spontaneous breaking of $SU(3)_C$ as the Universe cools and ending with its subsequent restoration. Although there have been studies of multistep phase transitions incorporating $SU(3)_C$ -breaking [7, 23, 25], only the last has gives a viable mechanism to break $SU(3)_C$ symmetry and restore it at zero temperature¹.

In this study, we follow the general set-up of Ref. [25] where $SU(3)_C$ -breaking is induced by colored scalars obtaining a vacuum expectation value (vev) during the first transition, which breaks both the color $SU(3)_C$ and electroweak (EW) $SU(2)_L \times U(1)_Y$ symmetries of the SM. This vev is then erased during the subsequent transition to the present “Higgs phase”, wherein the only the neutral component of the Higgs doublet obtains a vev. We refer to these two transitions as the CoB and EW phase transitions, respectively (though technically both break EW symmetry). We develop a full working scenario of baryogenesis under these conditions, which we refer to

*Electronic address: mjrm@physics.umass.edu

†Electronic address: graham.white@monash.edu

‡Electronic address: pwinslow@physics.umass.edu

¹ We note that ref [25] did not analyse the strength of the phase transition or which parts of the parameter space have sufficiently fast tunnelling. A detailed investigation into color breaking phase transitions is the subject of ongoing research.

as color-breaking baryogenesis (CoBBG). We will focus our attention on the CP violation and charge transport dynamics and not the dynamics of the phase transition that was previously studied in Ref. [25].

To demonstrate this new paradigm, we introduce two new scalar fields, $C_{1,2}$, that are charged under $SU(3)_C$ as well as $SU(2)_L \times U(1)_Y$. In order to prevent the existence of stable colored relics, we take these fields to interact with the Standard Model (SM) as leptoquarks through Yukawa-type interactions. With this field content, the thermal history of symmetry breaking is

$$\begin{aligned} & SU(3)_C \times SU(2)_L \times U(1)_Y \\ \xrightarrow{T_1} & SU(2)_C \times U(1)_{X_1} \times U(1)_{X_2} \\ \xrightarrow{T_2} & SU(3)_C \times U(1)_{EM} \quad , \end{aligned} \quad (2)$$

where $X_{1,2}$ denote two independently conserved $U(1)$ charges during the CoB phase that accompany a residual color $SU(2)_C$ symmetry. The BAU is generated during the first phase transition at temperature T_1 , with the Sakharov conditions realized as follows:

1. Baryon number conservation is violated in two ways: the usual electroweak sphalerons anomalously violating $B + L$ and spontaneous violation of $B - L$ in the color breaking phase, since the leptoquark fields C_j carry $B - L$.
2. The leptoquark-quark-lepton Yukawa couplings contain new CP-violating complex phases that source the generation of charge asymmetries during the first transition.
3. The spontaneous breaking of $SU(3)_C$ symmetry proceeds via a strongly first order phase transition, resulting in nucleation of CoB bubbles and, thereby, satisfying the out-of-equilibrium requirement.

During the second transition at temperature T_2 , the BAU produced during the first step inside the CoB phase is transferred to the Higgs phase. So long as the second transition does not permit re-excitation of the unbroken phase EW sphalerons or injection of significant entropy, the first phase BAU will not be washed out or diluted when the second transition occurs.

During the first step, the BAU produced via electroweak sphalerons is directly analogous to EWBG. Electroweak sphalerons are unsuppressed in the symmetric phase. CP violating interactions with the walls of the expanding CoB phase bubbles creates a total left handed number density that biases the sphalerons at the bubble exteriors. This produces a net $B + L$ asymmetry, some of which is swept up by the advancing bubble wall. For a sufficiently strong first order CoB transition, the broken phase EW sphaleron transitions will be sufficiently quenched by the C_j vevs so as to preclude washout of the $B + L$ asymmetry.

The second mechanism for violating baryon number conservation involves the spontaneous violation of $B - L$ number conservation by the C_j vevs. The total $B - L$ inside and outside the bubble is zero, however a non-zero $B - L$ density is trapped inside the expanding bubble. The size of this contribution however is negligible as the $B - L$ density relaxes to zero within a trillionth of the Hubble length at the time of nucleation and will continue to diffuse. On the other hand, the $B + L$ asymmetry is effectively conserved deep within the color broken phase and persists into the electroweak phase. The net BAU is, thus, dominated by the conventional $B + L$ generating EWBG mechanism. We find that given the present phenomenological constraints from collider searches and EDMs, the resulting BAU can be comparable in magnitude to the observed asymmetry.

We organize our discussion of this scenario as follows. In the Section II we define our exact choice of model to illustrate this scenario and section III elaborates on the symmetry breaking patterns associated with the multi-step phase transition. In Section IV we analyze all issues of charge transport including local equilibrium considerations, derivation of quantum transport equations, and our results including the contribution from the electroweak mechanism. Section V discusses the zero temperature phenomenology before we conclude in Section VI.

II. THE MODEL

Our illustrative model consists of the SM plus two scalar leptoquark fields, $C_{1,2}$, that must be charged under $SU(3)_C$ and $SU(2)_L$ in order to catalyze a CoB phase transition and quench electroweak sphalerons during this transition. In general, there are three scalar leptoquark representations that couple to SM fermions and have non-trivial $SU(2)_L$ quantum numbers [28], $(3,3)_{-1/3}$, $(3,2)_{7/6}$, and $(3,2)_{1/6}$. We seek a model that has the minimum number of free parameters, is least constrained phenomenologically, and does not enable any baryon number violating processes at zero temperature.

The $(3,3)_{-1/3}$ representation does not pass these requirements as it couples to both $Q_L Q_L$ and $Q_L^\dagger L_L^\dagger$, violating baryon number explicitly at tree level. The $(3,2)_{7/6}$ representation admits an enhanced $\mu \rightarrow e\gamma$ rate by virtue of it coupling to both $Q_L^\dagger e_R$ and $u_R^\dagger L_L$. The same enhancement also appears in 1-loop logarithmically divergent contributions to the charged lepton mass matrix, leading to non-trivial naturalness constraints even if the leptoquarks only couples to third generation particles [29]. In contrast, the $(3,2)_{1/6}$ representation only couples to $d_R^\dagger L_L$, so it is not subject to the above phenomenological constraints. Furthermore it has no perturbative baryon number violation and can catalyze gauge coupling unification [30]. We therefore use this representation to illustrate the mechanism of CoBBG.

Given the quantum numbers of the $C_{1,2}$ fields, we denote them as

$$C_{j\alpha} = \begin{pmatrix} \chi_{j\alpha}^{2/3} \\ \chi_{j\alpha}^{-1/3} \\ \chi_{j\alpha} \end{pmatrix} \quad j = 1, 2 \quad (3)$$

where Roman and Greek subscripts indicate the field and $SU(3)_C$ indices respectively, while superscripts represent the electromagnetic charges of the $SU(2)_L$ component fields. The most general Yukawa interaction for this representation is

$$\mathcal{L}_Y \supset \bar{d}_R^\alpha (Y^1 C_{1\alpha} + Y^2 C_{2\alpha}) L + h.c. \quad (4)$$

where flavor indices have been suppressed and the $SU(2)_L$ contraction is

$$C_{j\alpha} L \equiv \chi_{j\alpha}^{2/3} e_L - \chi_{j\alpha}^{-1/3} \nu_L. \quad (5)$$

The 3×3 Yukawa matrices, Y^1 and Y^2 , couple right handed down-type quarks (d_R, s_R, b_R) to left handed leptons (e_L, μ_L, τ_L) and neutrinos ($\nu_{eL}, \nu_{\mu L}, \nu_{\tau L}$). These new Yukawa matrices are arbitrary. However, the absence of large flavor changing neutral currents (FCNC) combined with LHC constraints being significantly more stringent for leptoquarks coupled to first or second generation fermions [31] suggests a hierarchical structure where $\bar{b}_R - \nu_{\tau L}$ couplings are dominant. Consequently, we take

$$Y^i = \text{diag}(0, 0, \tilde{y}_i), \quad (6)$$

where the zeros here indicate sub-leading couplings that we neglect in our analysis. Consequently, there is only one rephasing invariant CP phase and it is the relative phase $\text{Im}(\tilde{y}_1^* \tilde{y}_2)$. This is the minimum structure necessary to illustrate the CoBBG mechanism.

Note that in Ref. [25] it was found that in order to have a phenomenologically viable scenario where color symmetry is broken and restored, one requires there to be gauge singlets in the model. The gauge singlet allows the leptoquark mass to be a TeV or higher and can result in the leptoquark mass during the color breaking phase to substantially differ from its zero temperature value in the standard model phase. In this paper we ignore gauge singlets and leave such features to future work.

III. SPONTANEOUS SYMMETRY BREAKING OF $SU(3)_C \times SU(2)_L \times U(1)_Y$

In this section, we describe the pattern of spontaneous symmetry breaking during the multistep phase transition. It is necessary to understand this pattern as the presence of conserved gauge symmetries during the CoB phase will be used to make significant simplifications in the next section.

Without loss of generality, we choose the orientation of the color breaking vevs such that the shifted C_j fields are

$$\begin{pmatrix} \chi_{j\alpha}^{2/3} \\ \chi_{j\alpha}^{-1/3} \\ \chi_{j\alpha} \end{pmatrix} \rightarrow \begin{pmatrix} \chi_{j\alpha}^{2/3} \\ \varphi_j \delta_\alpha^3 + \sigma_{j\alpha}^{-1/3} \\ \chi_{j\alpha} \end{pmatrix} \quad j = 1, 2 \quad (7)$$

where φ_j are the vevs and the δ_α^3 singles out a direction in $SU(3)_C$ space. In order to identify the symmetry breaking pattern, we examine the gauge boson mass spectrum in the CoB phase.

Neglecting fluctuations around the vevs, the gauge boson mass spectrum is given by

$$\begin{aligned} \sum_j |D_\mu \langle C_{j\alpha} \rangle|^2 &= \varphi_{CB}^2 \\ &\times \left[e_S^2 (G_\mu^{+,45} G_\mu^{-,45} + G_\mu^{+,67} G_\mu^{-,67}) + e_W^2 W_\mu^+ W_\mu^- \right. \\ &\left. + (W_\mu^3 \ B_\mu \ G_\mu^8) \frac{\mathcal{M}^2}{2} \begin{pmatrix} W_\mu^{3\mu} \\ B_\mu \\ G_\mu^{8\mu} \end{pmatrix} \right] \end{aligned} \quad (8)$$

where $\varphi_{CB}^2 \equiv \varphi_1^2 + \varphi_2^2$ and the hypercharge, weak, and strong gauge couplings have been normalized as

$$(e_Y, e_W, e_S) \equiv (g_Y/\sqrt{2}, g_W/\sqrt{2}, g_S/\sqrt{2}). \quad (9)$$

The $G_\mu^{\pm,ij} \equiv \frac{1}{\sqrt{2}} (G_\mu^i \mp iG_\mu^j)$ fields correspond to the well-known $SU(3)_C$ generators of isospin ($ij=12$), U-spin ($ij=45$), and V-spin ($ij=67$) while the $W^\pm \equiv \frac{1}{\sqrt{2}} (W_\mu^1 \mp iW_\mu^2)$ fields correspond to the familiar generators of weak isospin.

The 3×3 mass matrix takes the form

$$\mathcal{M}^2 = \begin{pmatrix} e_W^2 & -\frac{e_W e_Y}{3} & \frac{2e_W e_S}{\sqrt{3}} \\ -\frac{e_W e_Y}{3} & e_Y^2 & -\frac{2}{3\sqrt{3}} e_S e_Y \\ \frac{2e_W e_S}{\sqrt{3}} & -\frac{2}{3\sqrt{3}} e_S e_Y & \frac{4}{3} e_S^2 \end{pmatrix}. \quad (10)$$

This matrix has only one non-zero eigenvalue, implying the presence of two unbroken and one broken $U(1)$ gauge symmetries present in the CoB phase. We denote the corresponding three mass eigenstate fields as

$$(X_{1\mu}, X_{2\mu}, X_{3\mu})^T = \mathcal{U} (W_\mu^3, B_\mu, G_\mu^8)^T \quad (11)$$

where \mathcal{U} diagonalizes \mathcal{M}^2 . While $X_{1\mu}$ and $X_{2\mu}$ remain massless, mediating long-range forces associated with the unbroken symmetries $U(1)_{X_1}$ and $U(1)_{X_2}$, $X_{3\mu}$ develops a mass

$$m_{X_3}^2 = \varphi_{CB}^2 / 9 (12e_S^2 + 9e_W^2 + e_Y^2) \quad (12)$$

and thus mediates a short-range force associated with the broken $U(1)_{X_3}$ symmetry. The corresponding charge

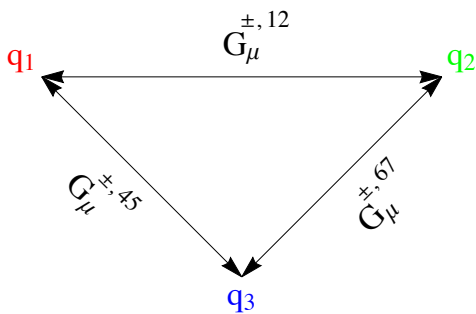


FIG. 1: The interaction pattern of gauge fields corresponding to $SU(3)_C$ generators of isospin ($G_\mu^{\pm,12}$), U-spin ($G_\mu^{\pm,45}$), and V-spin ($G_\mu^{\pm,67}$) and fields in the fundamental triplet representation.

generators of these U(1) symmetries are given by

$$\begin{aligned} Q_{X_1} &= T^8 - \frac{2}{\sqrt{3}}\tau^3 \\ Q_{X_2} &= \tau^3 + 3Y \\ Q_{X_3} &= T^8 + \frac{\sqrt{3}}{2} \frac{e_W^2}{e_S^2} \tau^3 - \frac{1}{2\sqrt{3}} \frac{e_Y^2}{e_S^2} Y. \end{aligned} \quad (13)$$

The charges Q_{X_1} and Q_{X_2} are conserved in both the symmetric and color broken phase. The gauge fields corresponding to the $SU(3)_C$ isospin generators are missing from Eq. (8) and thus remain massless, indicating the existence of an unbroken $SU(2)_C$ subgroup of $SU(3)_C$ in the CoB phase. This situation effectively distinguishes color state q_3 from q_1, q_2 , indicating that its' dynamics should be treated separately in the CoB phase. This situation is represented graphically in Fig. 1 and further clarified in Section IV A. In Section IV B, we will study the charge transport dynamics of each independent color separately.

IV. BARYOGENESIS

The BAU calculation is performed in two steps. First, we analyze charge transport dynamics of the relevant number densities in order to calculate the space time varying $B - L$ and chiral charge densities generated during the strongly first-order CoB phase transition. Second, the total left handed number density that biases the sphalerons resulting in a $B + L$ asymmetry via the EWBG mechanism. Combining the results of contributions yields the net BAU in the CoB phase.

The dynamics of particle number densities during a first order phase transition is a highly non-Markovian process that depends on the entire history of the system. In particular, “memory effects” can lead to a resonant boost of both CP violating sources and CP conserving relaxation terms that result from interactions with the space time varying vacuum [32–35]. Recall that our model contains a new, $T = 0$ rephasing invariant the lep-quark interaction that results in a new CP-violating

(CPV) and $(B - L)$ -violating (BLV) source $S_i^{(\text{CPV}, \text{BLV})}$ for the transport equations

$$\partial_\mu j_i^\mu = - \sum_j \Gamma_{ij} \mu_j + S_i^{(\text{CPV}, \text{BLV})} \quad (14)$$

where j_i^μ and μ_i are the charge current density and chemical potential, respectively, of particle species i and Γ_{ij} are the rates of interactions between species i and j .

The computation of the $S_i^{(\text{CPV}, \text{BLV})}$ is, in general, quite subtle, and there remain a number of open theoretical issues for the CPV-sources involving fermions (for a discussion, see *e.g.*, Ref. [11] and references therein). The general framework we adopt is the Schwinger-Keldysh closed time path formalism [36–41]. We will work with the vev insertion approximation (VIA), wherein we treat space-time varying vevs appearing in the b - ν mass matrix perturbatively to lowest non-trivial order. The diagrammatic representation of $S_i^{(\text{CPV}, \text{BLV})}$ in the VIA is shown Fig. 2. We expect that the VIA gives a reasonable guide to the magnitude of the CPV effects and allows one to see structure of the dynamics in our scenario. A more refined treatment including full accounting for flavor oscillations and vev-resummations is in progress[33, 34, 42, 43], and it remains unclear as to whether the VIA yields an overestimate or underestimate. Consequently, we will take our results as indicative of the magnitude of the BAU in our set up and not as numerically definitive.

With these caveats in mind, we apply the techniques in Ref. [35, 44], we obtain

$$\begin{aligned} S_b^{(\text{CPV}, \text{BLV})} &= -S_{\nu_L}^{(\text{CPV}, \text{BLV})} = \\ &= \frac{\text{Im}[\tilde{y}_1 \tilde{y}_2]}{\pi^2} v_{CB}^2(z) \frac{\partial \zeta(z)}{\partial t} \int_0^\infty \frac{k^2 dk}{\omega_{\nu_L} \omega_b} \\ &= \text{Im} \left[(\mathcal{E}_{\nu_L} \mathcal{E}_b + k^2) \left(\frac{n_f(\mathcal{E}_{\nu_L}) + n_F(\mathcal{E}_b)}{(\mathcal{E}_{\nu_L} + \mathcal{E}_b)^2} \right) \right. \\ &\quad \left. + (\mathcal{E}_{\nu_L} \mathcal{E}_b^* - k^2) \left(\frac{n_f(\mathcal{E}_{\nu_L}) - n_F(\mathcal{E}_b^*)}{(\mathcal{E}_b^* - \mathcal{E}_{\nu_L})^2} \right) \right]. \end{aligned} \quad (15)$$

Here $\tan \zeta(z)$ is the ratio of the vevs of the colored scalars, $\varphi_2(z)/\varphi_1(z)$, n_F is the Fermi-Dirac distribution function, $\omega_i = \sqrt{k^2 + m_i^2}$, and $\mathcal{E}_i \equiv \sqrt{k^2 + m_i^2} - i\Gamma_i$ with m_i and Γ_i representing the fully corrected thermal mass² and width of state i ³.

Denoting the chemical potentials of the left handed tau neutrino and the third color-component of the right handed bottom quark as $\mu_{\nu_{\tau L}}$ and μ_{b_3} , respectively, we

² for a more detailed treatment of thermal masses in phase transitions see [45]

³ In principle, one can have CP violating sources resulting from CP violation in the scalar potential, *e.g.*, see [46]. However, for the purposes of this paper, we only consider the CP violating source listed in Eq. (15).

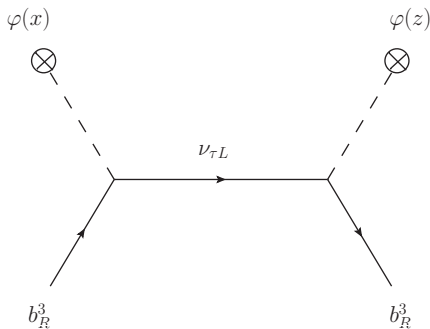


FIG. 2: Interaction between the left handed tau neutrino and the right handed 3rd color bottom quark with space-time varying vacuum. This interaction is responsible for new CP violating source

can write the CP conserving relaxation term associated with Fig 2 as

$$S^{CP} = (\mu_{\nu_{\tau L}} - \mu_{b_R^3})\Gamma_M \quad (16)$$

with

$$\Gamma_M = \frac{|\tilde{y}_1\varphi_1(z) + \tilde{y}_2\varphi_2(z)|^2}{2\pi^2 T} \int_0^\infty \frac{k^2 dk}{\omega_\nu \omega_b}$$

$$\text{Im} \left[(\mathcal{E}_{\nu_L} \mathcal{E}_b + k^2) \left(\frac{h_F(\mathcal{E}_{\nu_L}) + h_F(\mathcal{E}_b)}{\mathcal{E}_{\nu_L} + \mathcal{E}_b} \right) - (\mathcal{E}_{\nu_L} \mathcal{E}_b^* - k^2) \left(\frac{h_F(\mathcal{E}_{\nu_L}) + h_F(\mathcal{E}_b^*)}{\mathcal{E}_b^* - \mathcal{E}_{\nu_L}} \right) \right]. \quad (17)$$

and

$$h_F(x) = e^{x/T} / (1 + e^{x/T})^2. \quad (18)$$

With these sources in hand, we now analyze the transport equations (14) in detail. A particle's dynamics are important if it is able to diffuse ahead of the advancing bubble wall. The diffusion time is characterized by a diffusion constant D_i (see below) and the bubble wall velocity v_w : $\tau_{\text{diff}} = D/v_w^2 \sim 10^4/T$ [47] for v_w on the order of 0.05. This time scale is typically shorter than the inverse rate for the EW sphalerons to convert the left-handed number density n_L into $B + L$, $\tau_{\text{EW}} \sim \Gamma_{\text{EW}}^{-1} \sim 10^5/T$, where $\Gamma_{\text{EW}} \approx 120\alpha_W^5 T$ and α_W is the $\text{SU}(2)_L$ fine structure constant[48]. Consequently, we may decouple the equations for n_L and $B + L$ generation to a reasonable approximation.

Following Refs. [35], we assume a planar bubble wall profile so that charge densities are functions only of their displacement $z = |\vec{x} - \vec{v}_w t|$ from the bubble wall in its rest frame, where \vec{x} is the co-ordinate in the plasma rest frame and where the $z < 0$ ($z > 0$) region corresponds to the (un)broken phase. We also apply Fick's law to

make the replacement $j_i^\mu \equiv (n_i, \vec{j}_i) \rightarrow (n_i, -D_i \vec{\nabla} n_i)$. Here, n_i is the charge density and D_i is the diffusion constant which describes how n_i is transported away from the bubble wall. Assuming $\mu_i/T \ll 1$, the chemical potentials are related to the charge densities as $n_i = (T^2/6)k_i\mu_i + \mathcal{O}(\mu_i/T)^3$ where the k_i factor counts the effective degrees of freedom of species i in the plasma. These k_i factors are

$$k_i = g_i \frac{6}{\pi^2} \int_{m_i/T}^\infty dx x \frac{e^x}{(e^x \pm 1)^2} \sqrt{x^2 - m_i^2/T^2} \quad (19)$$

where g_i counts the number of internal degrees of freedom for species i and m_i is the effective mass of particle i at temperature T . By searching for steady-state solutions that only depend on z , we can make the replacements $\partial n_i(z)/\partial t \rightarrow v_w n_i'(z)$ and $\vec{\nabla}^2 n_i(z) \rightarrow n_i''(z)$ where the prime denotes differentiation with respect to z and $v_w \equiv \partial z/\partial t$ is the velocity of the bubble wall. After these modifications, the Boltzmann equations become a coupled set of second order differential equations for the charge densities $n_i(z)$ with one such equation for each independent particle species coupled to the baryon- and CP-violating source in the plasma.

A. Local Equilibrium Considerations

The spontaneous breaking of $\text{SU}(3)_C$ symmetry implies that one needs to consider the transport dynamics of each color separately. A significant simplification can be made if the dynamics of colour and weak isospin singlet can be separated from multiplets. This is what we endeavor to achieve in this section. The only assumption we will require is that we are in a section of parameter space where gauge interactions are fast enough compared to the inverse of the diffusion rate which is controlled by the velocity of the advancing bubble wall, $\Gamma_D \sim v_W^2/D$ [49]. For the sake simplicity we will also assume that scalar interactions involving both colored scalars are also fast enough compared to a diffusion rate to equilibrate the two

$$n_Q = \sum_i n_{t_{Li}} + n_{b_{Li}}$$

$$n_T = \sum_i n_{t_{Ri}}$$

$$n_B = \sum_i n_{b_{Ri}}$$

$$n_U = \sum_i n_{c_{Ri}}$$

$$n_L = n_{\tau L} + n_{\nu_{\tau L}}$$

$$n_H = n_{H^+} + n_{H^0}$$

$$n_C = \frac{1}{2} \left(\sum_{i\alpha} n_{\chi_{i\alpha}^{2/3}} + n_{\chi_{i\alpha}^{-1/3}} \right) \quad (20)$$

where the above species are the left handed third generation quark doublet, the right handed top, bottom and charm, the third generation left handed lepton doublet, the Higgs doublet and the combined colored scalar densities respectively. Note that $i \in (1, 2, 3)$ is an $SU(3)_C$ index and $\alpha \in (1, 2)$ is an index for the species of leptoquark.

Let us begin with making use of gauge interactions. We will denote the chemical potentials of the two components of an arbitrary $SU(2)_L$ doublet as μ_\uparrow and μ_\downarrow respectively. Also let us denote the three components of an arbitrary color triplet as μ_i for $i \in 1, 2, 3$. The remaining $SU(2)_C$ symmetry results in a local equilibrium relation between the first two colors

$$\mu_1 = \mu_2 . \quad (21)$$

The result of this is that there are only two independent colors. We can therefore write all components of the $SU(3)_C$ triplet can be written as a linear combination of the color singlet and octet state which we denote as μ_8 and μ_S respectively

$$\begin{pmatrix} \mu_S \\ \mu_8 \end{pmatrix} = \begin{pmatrix} 2 & 1 \\ \frac{1}{\sqrt{3}} & -\frac{1}{\sqrt{3}} \end{pmatrix} \begin{pmatrix} \mu_{1,2} \\ \mu_3 \end{pmatrix} \quad (22)$$

where $\mu_{1,2}$ represents either color since they are in equilibrium.

The assumption of local gauge equilibrium for massive gauge results in the following relations between chemical potentials

$$\begin{aligned} \mu_1 - \mu_3 &= \frac{1}{\sqrt{3}}\mu_8 = \mu_{G_{45}} \\ \mu_2 - \mu_3 &= \frac{1}{\sqrt{3}}\mu_8 = \mu_{G_{67}} \\ \mu_\uparrow - \mu_\downarrow &\equiv \Delta\mu = -\mu_W \quad , \end{aligned} \quad (23)$$

where μ_\uparrow (μ_\downarrow) denotes the chemical potential for any weak isodoublet with third component $+1/2$ ($-1/2$). The first two lines in Eq. (23) imply

$$\mu_{G_{45}} = \mu_{G_{67}} \equiv \mu_G \quad (24)$$

Similarly any chemical potential of the form $\Delta\mu$ is equal to $-\mu_W$. Therefore, the densities of all gauge multiplets in the network of transport equations for color and $SU(2)_L$ singlets can be written in terms of massive gauge bosons densities.

Next, we use the CoB phase conservation laws to eliminate the massive gauge boson densities from all transport equations for color and $SU(2)_L$ singlets. Recall from section III that there are the two charges $Q_{X_{1,2}}$ are conserved in the CoB phase. To make use of a conservation law one must set the sum of the charge asymmetry for all particle species to zero. For example, in the case of the Q_{X_1} conservation we have

$$\sum_{i \in \text{particles}} Q_{X_1} \left(\frac{6n_i}{T^2} \right) = \sum_{i \in \text{particles}} Q_{X_1} \mu_i k_i = 0 . \quad (25)$$

For convenience the relevant charges of all important particle species are given in the appendix. We find for Q_{X_1} the simple relationship

$$\mu_G = -\mu_W . \quad (26)$$

This allows us to eliminate the μ_G in terms of μ_W . Next we consider Q_{X_2} conservation. Using Eqs. (23), (24) and (26) we obtain

$$\mu_W = \frac{3}{16} \left(\frac{1}{6}\mu_{Q_L} + \frac{2}{3}\mu_{t_R} - \frac{1}{3}\mu_{b_R} - \frac{1}{2}\mu_L + \mu_H + \frac{2}{3}\mu_C \right) , \quad (27)$$

which can be used to eliminate μ_W . We have now achieved our goal of writing μ_8 and $\Delta\mu$ in terms of gauge singlet densities.

There exists one additional relationship that allows us to eliminate one more chemical potential. In the CoB phase, the scalar fluctuations about the CoB VEVs are real scalars that can no longer carry any charge, implying vanishing of their chemical potentials,

$$\mu_{\chi_{\alpha 3}^{-1/3}} = 0 \quad (28)$$

with $\alpha \in (1, 2)$ denoting the leptoquark species. Using equations (22), (23), (24) and (26) we can derive the relation

$$\mu_C = -7\mu_W . \quad (29)$$

Substituting into Eq. (27) and solving for μ_C allows us to eliminate the leptoquark chemical potential in favor of the quark, lepton, and Higgs chemical potentials appearing in Eq. (27). Thus, the final set of Boltzmann equations need not contain either μ_W or μ_C .

To conclude this section we briefly comment on the strong sphaleron rate. Strong sphalerons transitions convert left handed quarks into right handed quarks and vice versa. Since we are breaking $SU(3)_C$ through a strongly first order phase transition, the sphaleron rate for the third color gets suppressed in the CoB phase by a factor controlled by the sphaleron energy, $\Gamma_{\text{sph}} \sim \exp[-E_{\text{sph}}/T]$, where the sphaleron energy itself is proportional to the color breaking vev, v_{cb} . Therefore we can ignore strong sphaleron transitions for the third color. The linear combination of chemical potentials that multiply the remaining $SU(2)_C$ sphaleron rate $\Gamma_{SS}^{(2)}$ in the transport equations is just

$$\mu_{L1} + \mu_{L2} - \mu_{R1} - \mu_{R2} . \quad (30)$$

Using Eqs. (22) and (23), one finds that the contributions from the color octets cancel. Recall that we assume that local baryon number is conserved for the first two generations of particles. The result is that the Eq. (30) can be written in the form

$$\mu_{Li} - \mu_{Ri} = 2(8\mu_U + \mu_T + \mu_B - 2\mu_Q) . \quad (31)$$

B. Quantum Transport Equations

We now derive the Boltzmann equations for all relevant color and $SU(2)_L$ singlets. To that end, we first construct the Boltzmann equations for the color and isospin components of each field, adding them together to obtain the equations for the color and $SU(2)_L$ singlet densities. To illustrate, consider the right handed b -quark singlet charge density n_B . Following the steps laid out in the previous subsection we obtain the following equations for the two independent charge densities $n_{b_R^1}$ and $n_{b_R^3}$

$$\begin{aligned} \partial_\mu j_{b_R^1}^\mu &= -2\Gamma_{\chi^{2/3}} \left(\mu_{b_R^1} - \mu_{\chi_1^{2/3}} - \mu_{\tau_L} \right) \\ &\quad - 2\Gamma_{\chi^{-1/3}} \left(\mu_{b_R^1} - \mu_{\chi_1^{-1/3}} - \mu_{\nu_{\tau_L}} \right) \end{aligned} \quad (32a)$$

$$\begin{aligned} &- \Gamma_{SS}^{(2)} \sum_{i=gen.} \left(\mu_{u_{iR}^1} + \mu_{d_{iR}^1} - \mu_{u_{iL}^1} - \mu_{d_{iL}^1} \right), \\ \partial_\mu j_{b_R^3}^\mu &= -2\Gamma_{\chi^{2/3}} \left(\mu_{b_R^3} - \mu_{\chi_3^{2/3}} - \mu_{\tau_L} \right) \\ &- 2\Gamma_{\chi^{-1/3}} \left(\mu_{b_R^3} - \mu_{\nu_{\tau_L}} \right) - \Gamma_M \left(\mu_{b_R^3} - \mu_{\nu_{\tau_L}} \right) \\ &\quad + S^{(CPV, BLV)} \end{aligned} \quad (32b)$$

where $\Gamma_{\chi^{2/3}}$, $\Gamma_{\chi^{-1/3}}$ are the 3-body rates stemming from the Yukawa interactions in Eq. (4) and $\Gamma_{SS}^{(2)}$ is the strong sphaleron rate associated with non-perturbative $SU(2)_C$ gauge interactions.

Since the gluons associated with $SU(2)_C$ only mediate interactions between the first two components of a $SU(3)_C$ triplet, the strong sphaleron interactions connected with $SU(2)_C$ have no effect on any charge densities corresponding to the third color. Both the 2-body CP-conserving rate Γ_M and the baryon- and CP-violating source term $S^{(CPV, BLV)}$ originate from the interactions with the CoB vev and thus only appear in Eq. (32b). Moreover, the chemical potential $\mu_{\chi_3^{-1/3}}$ has vanished due to the formation of CoB VEVs. As a consequence, the combination $\mu_{b_R^3} - \mu_{\nu_{\tau_L}}$ is relaxed by both 3-body, $\Gamma_{\chi^{-1/3}}$, and 2-body, Γ_M , interaction rates in Eq. (32b). The factors of two in front of the $\Gamma_{\chi^{2/3}}$ and $\Gamma_{\chi^{-1/3}}$ rates represent the contributions from both doublets C_1 and C_2 whose individual isospin components have been equilibrated by potential operators.

Before taking the singlet combination of Eqs. (32a,32b), we simplify them by assuming that all χ fields have the same mass, implying that all 3-body rates are equal up to the (relatively negligible) difference between the τ_L and ν_{τ_L} thermal masses, *i.e.*, $\Gamma_{\chi^{2/3}} = \Gamma_{\chi^{-1/3}} \equiv \Gamma_C$. The singlet combination is

$$\begin{aligned} \partial_\mu j_B^\mu &\equiv 2\partial_\mu j_{b_R^1}^\mu + \partial_\mu j_{b_R^3}^\mu \\ &= - \left(\frac{1}{6} (\Gamma_C + \Gamma_M) (2\mu_B - \mu_C - 3\mu_L) \right. \\ &\quad \left. + \frac{2}{3} \Gamma_{SS}^{(2)} (8\mu_U + \mu_T + \mu_B - \mu_Q) \right) + S^{(CPV, BLV)} \end{aligned} \quad (33)$$

where $\mu_C \equiv \sum_\alpha (\mu_{\chi_\alpha^{2/3}} + \mu_{\chi_\alpha^{-1/3}})$. Here, we have taken advantage of all equilibrium relations derived in section IV A to write the right hand side of Eq. (33) entirely in terms of weak isospin and color singlets. Note that to this point we have factored out a factor of 3(2) from the k-factors to account for the components of color triplets (isospin doublets). We now reabsorb these factors into the k-factors appearing in our Boltzmann equations. The final form then becomes

$$\begin{aligned} v_w B' - D_q B'' &= -(\Gamma_C + \Gamma_M) \left(\frac{B}{k_B} - \frac{C}{k_C} - \frac{L}{k_L} \right) \\ &\quad + 2\Gamma_{SS}^{(2)} \left(\frac{8U}{k_U} + \frac{T}{k_T} + \frac{B}{k_B} - \frac{2Q}{k_Q} \right) + S^{(CPV, BLV)}, \end{aligned} \quad (34)$$

where we have expressed the left hand side of the Boltzmann equation in terms of the singlet density as described in section IV.

Following the steps laid out above for all other independent charge densities in Eq. (20), we obtain

$$v_w U' - D_q U'' = -2\Gamma_{SS}^{(2)} \mathcal{E}_{SS} \quad (35a)$$

$$v_w T' - D_q T'' = -2\Gamma_{SS}^{(2)} \mathcal{E}_{SS} - \Gamma_H \mathcal{E}_H \quad (35b)$$

$$v_w Q' - D_q Q'' = 4\Gamma_{SS}^{(2)} \mathcal{E}_{SS} + \Gamma_H \mathcal{E}_H \quad (35c)$$

$$v_w H' - D_L H'' = \Gamma_H \mathcal{E}_H \quad (35d)$$

$$\begin{aligned} v_w B' - D_q B'' &= -2\Gamma_{SS}^{(2)} \mathcal{E}_{SS} - (\Gamma_C + \Gamma_M) \mathcal{E}_M \\ &\quad + S^{(CPV, BLV)} \end{aligned} \quad (35e)$$

$$v_w L' - D_L L'' = (\Gamma_C + \Gamma_M) \mathcal{E}_M - S^{(CPV, BLV)} \quad (35f)$$

$$\begin{aligned} \mathcal{E}_H &\equiv \left(\frac{T}{k_H} - \frac{Q}{k_Q} - \frac{H}{k_H} \right), \quad \mathcal{E}_M \equiv \left(\frac{B}{k_B} - \frac{C}{k_C} - \frac{L}{k_L} \right) \\ \mathcal{E}_{SS} &\equiv \left(\frac{8U}{k_U} + \frac{T}{k_T} + \frac{B}{k_B} - \frac{2Q}{k_Q} \right). \end{aligned} \quad (36)$$

where

$$C = -\frac{7}{10} \left(\frac{1}{6} Q + \frac{2}{3} T - \frac{1}{3} B - \frac{1}{2} L + H \right), \quad (37)$$

obtained through the combination of Eqs. (29) and (27).

Note that we have assumed the rate for EW sphalerons is much slower than all other rates considered thus far and have, thus, not included the EW sphaleron transition terms in computing the densities⁴. Consequently, the transport equations should conserve $B+L$. This conservation is manifest for the third generation fermions, as one can see by adding Eqs. (35b, 35c, 35e, 35f) and noting that the transport equation for the RH leptons has a vanishing RHS. For the first and second generation fermions,

⁴ We will take the resulting LH fermion density as input into the EW sphaleron-driven equation for $B+L$ below.

we note that (a) the transport equation for the first and second generation down-type RH quarks has the same form as Eq. (35a) but with $U \rightarrow D$; (b) the equation for the first and second generation LH quark doublets has the same form as Eq. (35c) but with vanishing Γ_H ; (c) the transport equations for the first and second generation LH and RH leptons also have a vanishing RHS. Consequently, $B + L$ is locally conserved for the first and second generations as well in the limit of vanishing EW sphaleron rate.

In Eqs. (35a,35b,35c,35e), the numerical value of the diffusion constant, D_q , for all quark states depends on whether $SU(3)_C$ or $SU(2)_C$ is the conserved color symmetry. However, for simplicity, we assume the value $D_q = 6/T$ throughout, obtained in $SU(3)_C$ conserving calculations, while for D_L we take $100/T$ [50, 51]

The set of transport coefficients excluding the relaxation term which was already given in Eq. (17) are

$$\Gamma_H = \frac{36y_t^2}{T^2} \mathcal{I}_F(m_{t_R}, m_Q, m_C) + 0.13\alpha_s T \quad (38)$$

$$\Gamma_C = \frac{144|\tilde{y}_1|^2}{T^2} \mathcal{I}_F(m_{b_R}, m_L, m_C) + 0.52|\tilde{y}_1|^2\alpha_s T. \quad (39)$$

The relaxation rates Γ_H and Γ_C depend on the function \mathcal{I}_F [52] that characterizes the three-body decays, $t_R \rightarrow Q + H$ and $b_R \rightarrow L + C$ respectively, and a 4-body scattering contribution proportional to α_s . Note that in regions of mass parameter space where \mathcal{I}_F due to kinematic blocking, the 4-body term remains non-zero. Also note that for the sake of simplicity we have restricted ourself to the case where $\tilde{y}_1 = \tilde{y}_2$.

Finally, we consider the non-perturbative $SU(2)_C$ strong sphaleron rate $\Gamma_{SS}^{(2)}$. In Ref. [53], the N_C dependence of the strong sphaleron rate was explored. By following their results, we identify the numerical value of the $SU(2)_C$ strong sphaleron rate to be roughly $\Gamma_{SS}^{(2)} \simeq 9\alpha_s^4 T$.

In the next section, we present our solution of the Boltzmann equations and discuss how this is related to the determination of Y_B in CoBBG.

C. Solving the Quantum Transport Equations and Results

We begin by discussing the parameterization of the set of Boltzmann equations. In principle, the numerical values of all coefficients and source terms in Eq. (35f) are parameterized by 6 unknown model parameters: two tree level masses ($m_H(T), m_C(T)$) and two complex Yukawa couplings (\tilde{y}_1, \tilde{y}_2). However, only the relative phase, δ , is physically relevant. Moreover, for simplicity, we assume that both Yukawa couplings have equal magnitudes $\tilde{y} \equiv |\tilde{y}_1| = |\tilde{y}_2|$. Under these assumptions, the prefactors in

Eqs. (15) and (16) become

$$\begin{aligned} \text{Im}(\tilde{y}_1 \tilde{y}_2^*)(\varphi_1 \dot{\varphi}_2 - \varphi_2 \dot{\varphi}_1) &= \tilde{y}^2 \sin \delta \dot{\zeta} \varphi_{CB}^2 \\ \text{and} \\ |\tilde{y}_1 \varphi_1 + \tilde{y}_2 \varphi_2|^2 &= \tilde{y}^2 \varphi_{CB}^2 (1 + \sin(2\zeta) \cos \delta) \end{aligned} \quad (40)$$

respectively, where we remind the reader that $\varphi_{CB}^2 = \varphi_1^2 + \varphi_2^2$ and $\tan \zeta = \varphi_2/\varphi_1$.

The first step in determining Y_B in CoBBG is to solve the Boltzmann equations in Eq. (35f). We note that, without a source term for any of the T , Q , or U densities, there exists a linear combination of their Boltzmann equations for which the right hand side vanishes, *i.e.*,

$$v_w(T' + Q' + U') - D_q(T'' + Q'' + U'') = 0. \quad (41)$$

Each of these densities diffuse in the plasma at the same rate which implies that this combination is locally conserved. This means that

$$T + Q + U = 0, \quad (42)$$

thereby eliminating the need for explicit retention of the transport equation for $U = -(Q + T)$. We then employ the novel methods of Ref. [54] to directly solve the reduced set of five Boltzmann equations analytically without recourse to any assumption about the size of the 3-body rates.

For each of the densities, $\mathbb{D} = \{T, Q, H, B, L\}$, we assume the boundary conditions $\mathbb{D}(\pm\infty) = 0$. That is, we assume that the electroweak phase transition in which $SU(3)_C$ is restored occurs at a time much larger than the diffusion time scale τ_D . For simplicity we also approximate the relaxation rate Γ_M near the bubble wall as a step function

$$\Gamma_M(z) = \begin{cases} 0 & z < 0 \text{ (unbroken)} \\ \Gamma_M(10L_w) & z > 0 \text{ (broken)} \end{cases}, \quad (43)$$

where L_w is the width of the bubble wall and $10L_w$ is simply a sufficient distance from the wall that Γ_M has become constant in the CoB phase. This produces a slight underestimate of the baryon asymmetry, however the error tends to be small [54]. In order to determine the numerical values of Γ_M and $S^{(\text{CPV, BLV})}$ we further require the full spacetime dependence of the CoB vev φ_{CB} and its angle $\tan \zeta$ across the bubble wall. A detailed calculation of this dependence requires an involved analysis of the full scalar potential, which we defer to future work. For simplicity, we assume a kink profile [55–58]

$$\begin{aligned} v_{CB}(z) &= \frac{\xi T}{2\sqrt{2}} \left(1 + \tanh \left(2\alpha \frac{z}{L_w} \right) \right) \\ \zeta(z) &= \frac{\Delta\zeta}{2} \left(1 + \tanh \left(2\alpha \frac{z}{L_w} \right) \right) \end{aligned} \quad (44)$$

where we take $\alpha = \xi = 3/2$. Following detailed calculations in the MSSM [59], we assume a conservative value

for $\Delta\zeta \equiv \zeta(T)|_{z \rightarrow \infty} - \zeta(T)|_{z \rightarrow -\infty}$ which we take to be $\Delta\zeta = 0.01$. Note that the BAU is directly proportional to $\Delta\zeta$ and the presence of scalar singlets can lift the value of $\Delta\zeta$ by an order of magnitude or more [60].

In Fig. 3, we present the charge densities for the case of a maximal CP-violating phase, $\sin\delta = 1$, a Yukawa coupling of $\tilde{y} = 0.1$, and tree-level masses of $m_C(T) = 250$ GeV and $m_H(T) = 100$ GeV. Moreover, to obtain these results we have used the following phase transition parameters $T = 250$ GeV, $L_w = 10/T$, and $v_w = 0.05$.

We now discuss calculation of the total baryon asymmetry in the CoB phase. As previously stated, the baryon asymmetry has two components. A space time varying asymmetry in $B - L$ due to the spontaneous violation of this conserved number within the color broken phase and the usual component that arises from a total left handed number density which biases electroweak sphalerons ahead of the advancing bubble wall producing a net $B + L$ asymmetry. Note that deep within the color broken phase $B + L$ is effectively conserved and this asymmetry will persist into the electroweak phase.

In Fig. 4 and Fig. 5 we show how the baryon asymmetry varies as a function of spacetime for various values of the leptoquark tree level mass and coupling respectively. The dotted line in these figures are the contribution to the BAU from the electroweak mechanism whereas the solid line is the space time varying contribution from spontaneous breaking of $B - L$. The total $B - L$ is zero but there is a non-zero density inside the bubble. Note that the coordinate system is the rest frame of the bubble wall, the $B - L$ density is therefore trapped inside the bubble diluting as the bubble grows. We normalize the space time variable by the Hubble length at the time of nucleation to highlight that the $B - L$ contribution is very small. Generally we find that the space time varying $B - L$ density vanishes at about one trillionth of the Hubble length at the time of nucleation. A significant dilution of this already tiny contribution occurs by the time of recombination. From these figures we see that one can easily produce the BAU for a large range of parameter space during the color breaking phase transition. The BAU monotonically decreases with $m_C(T)/T$ but increases with \tilde{y} . The dependence on $m_C(T)/T$ is gentle indicating a weak dependence on the leptoquark mass. This is explained by the fact that the leptoquark masses do not enter the functions for the CPV sources, they only appear in the relaxation term Γ_C .

V. PHENOMENOLOGY

A. LHC constraints

At $T = 0$, the colored scalars, C_1 and C_2 , are produced through their strong interactions at the LHC. Under the assumption given in Eq. (6), the scalar decay

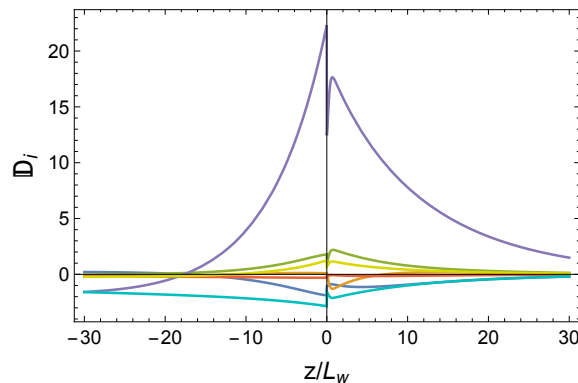


FIG. 3: Charge densities of all relevant species for $m_C(T) = 800$ GeV, $T = 250$ GeV, $m_H(T) = 100$ GeV, $\sin\delta = 1$, $\tilde{y} = 0.1$, $L_w = 10/T$ and $v_w = 0.05$. Region of positive (negative) z denotes the region of broken (unbroken) $SU(3)_C \times SU(2)_L$.

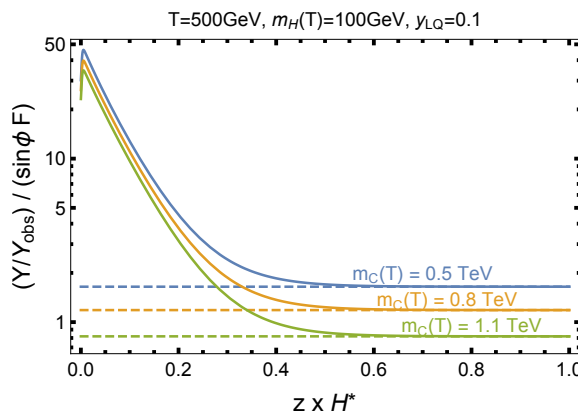


FIG. 4: Variation in BAU due to $m_C(T)$ as a function of the space time variable z normalized by the Hubble length. The BAU has two components: a space time varying component due to the spontaneous violation of baryon asymmetry and a component due to the EWBG mechanism. The space time varying component barely penetrates the bubble wall compared to the Hubble length.

modes are $\chi^{2/3} \rightarrow b_R\tau_L$ and $\chi^{-1/3} \rightarrow b_R\nu_{\tau L}$ with unit branching ratios. The CMS collaboration has recently placed limits on scalar leptoquarks which dominantly decay into these modes by studying their pair production. The dominant pair production mechanisms at the LHC for these colored scalars are through gluon-gluon fusion and quark-antiquark annihilation, for which the cross sections depend only on the scalar mass. At $\sqrt{s}=8$ TeV, limits have been derived on colored scalars decaying to $b_R\tau_L$ [61] using an integrated luminosity of 12.9 fb^{-1} . A unit branching ratio was assumed and upper limits on the production cross sections were set at the 95% C.L., yielding the bound of $m_{C_{2/3}} \geq 850$ GeV. Limits on leptoquarks decaying in the $b_R\bar{\nu}_\tau$ mode derived by the ATLAS collaboration are $m_{C_{-1/3}} \geq 640$ GeV [31].

Aside from direct searches, the colored scalars of CoBBG can also be searched for indirectly by exam-

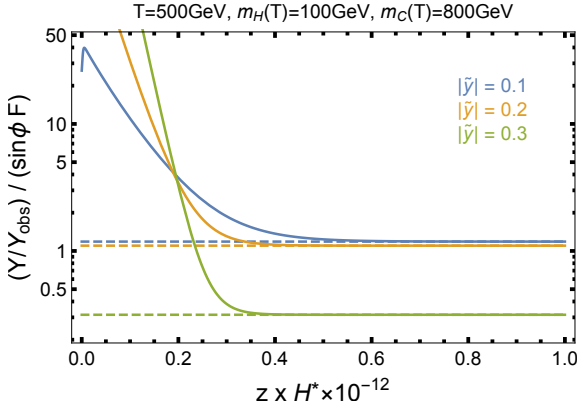


FIG. 5: Variation in BAU due to y_{LQ} as a function of the space time variable z normalized by the Hubble length. The BAU has two components: a space time varying component due to the spontaneous violation of baryon asymmetry and a component due to the EWBG mechanism. The space time varying component barely penetrates the bubble wall compared to the Hubble length.

ining their effects on the rates for production and decay of the SM Higgs. At the 1-loop level, their $SU(3)_C$ charges enable them to interfere with top quark loops in gluon-gluon fusion production of the SM Higgs. As well, their $U(1)_{EM}$ charges enable them to interfere with both top quark and W^\pm loops in Higgs-to-diphoton decay. The modifications of these rates are best expressed as ratios with the SM-valued rates, $R_{\gamma\gamma}(R_{gg}) \equiv \Gamma_{\gamma\gamma}/\Gamma_{\gamma\gamma}^{SM}(\sigma_{gg}/\sigma_{gg}^{SM})$. At leading, non-trivial order, one has

$$R_{\gamma\gamma} = \frac{|F_1(\tau_W) + \frac{4}{3}F_{1/2}(\tau_t) + N_c \sum_i Q_{EM}^2 \xi_{C_i} F_0(\tau_{C_i})|^2}{|F_1(\tau_W) + \frac{4}{3}F_{1/2}(\tau_t)|^2}$$

$$R_{gg} = \frac{|F_{1/2}(\tau_t) + \sum_i \xi_{C_i} F_0(\tau_{C_i})|^2}{|F_{1/2}(\tau_t)|^2}, \quad (45)$$

where we sum over the contributions of each colored scalar. Here, we have defined $\tau_i = 4m_i^2/m_h^2$,

$$\xi_{C_i} = 2 \frac{\lambda_{HC_i}}{g_1} \frac{M_W^2}{m_{C_i}^2}, \quad (46)$$

Q_{EM} is the electric charge of the scalar C_i , and all loop functions are defined in Ref. [62]. The parameters λ_{HC_i} are the couplings associated with the Higgs portal operator $H^\dagger H C_i^\dagger C_i$. While they do not directly enter the transport computation, they are nevertheless important for the phase transition dynamics.

Using these ratios, we construct the set of signal rates μ_{XX} associated with Higgs measurements, relative to pure SM-Higgs expectations, *i.e.*,

$$\mu_{XX} = \frac{\sigma \cdot \text{BR}}{\sigma^{SM} \cdot \text{BR}^{SM}}. \quad (47)$$

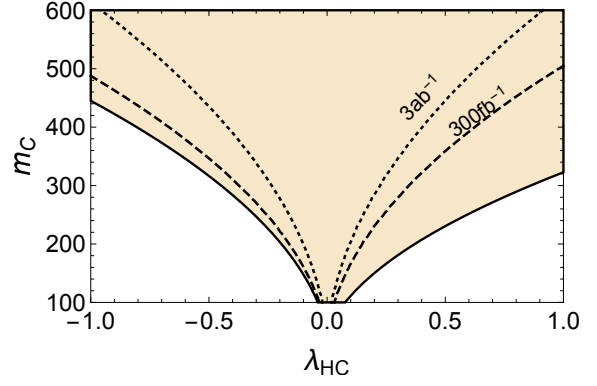


FIG. 6: Shaded region represents the allowed (m_C, λ_{HC}) parameter space from current LHC Higgs measurements at the 95% C.L. The dashed (dotted) line represents the 95% C.L. projected sensitivity to this parameter space at the 300fb^{-1} (3ab^{-1}) high luminosity LHC.

Each signal rate is a function of the Higgs portal couplings λ_{HC_i} and scalar masses m_{C_i} and, for simplicity, we assume that all scalars are degenerate in mass and share the same λ_{HC} . We then impose constraints on these parameters by performing a global χ^2 fit to the current Higgs data⁵ using

$$\chi^2(\lambda_{HC}, m_C) = \sum_X \left(\frac{\mu_{XX}^{obs} - \mu_{XX}}{\Delta\mu_{XX}^{obs}} \right)^2, \quad (48)$$

where μ_i^{obs} ($\Delta\mu_i^{obs}$) are the (uncertainties in the) observed signal rates. The resulting 95% C.L. limit on the parameters, shown in Fig. 6, implies that, for scalar masses above the current direct search limits ($m_C \gtrsim 500$ GeV), a wide range of λ_{HC} is open. We also include future projected limits expected from the HL-LHC [67–70], represented by the solid and dashed black contours in Fig. 6.

B. Electric Dipole Moments

Searches for permanent electric dipole moments (EDMs) provide constraints on the CP violating phases necessary for producing a baryon asymmetry (see, *e.g.*, Ref. [11] and references therein. For other recent EDM reviews, see [71–74] Here, we consider EDM constraints on the CP violating phases present in the leptoquark couplings, y_i . We find that improvements in experimental sensitivity by many orders of magnitude would be needed

⁵ aside from [63–65] which uses 13 TeV data, the most up to date signal strengths are taken from 7 and 8 TeV data in Ref. [66]. We use the 13 TeV signal strengths and uncertainties unless it is unavailable.

to probe the full parameter space of the specific CoB scenario discussed here.

We work in the effective field theory framework where weak scale particles, t , W^\pm , Z , H , and $C_{1,2}$ are considered heavy and integrated out. The effective Lagrangian that results from this is a sum of fermion EDMs, chromo-EDMs and the three-gluon Weinberg operator [75]

$$\begin{aligned} \mathcal{L}_{CPV} = & -\frac{i}{2}d_f\bar{f}\sigma^{\mu\nu}\gamma^5fF_{\mu\nu} - \frac{i}{2}\tilde{d}_qg_s\bar{q}_i\sigma^{\mu\nu}\gamma^5(T^a)_{ij}q_jG_{\mu\nu}^a \\ & + g_s\frac{C_W}{\Lambda^2}f^{abc}G_{\mu\nu}^a\tilde{G}^{b\nu\lambda}G_\lambda^{c\mu} + h.c. \end{aligned} \quad (49)$$

Here, $F_{\mu\nu}$ ($G_{\mu\nu}^a$) is the photon (gluon) field strength, $\tilde{G}_{\mu\nu}^a \equiv \frac{1}{2}\epsilon_{\mu\nu\alpha\beta}G^{\alpha\beta}$ is the dual field strength (with $\epsilon_{0123} = +1$), and T^a and f^{abc} are the full $SU(3)_C$ generators and structure constants, respectively. Finally Λ is the BSM scale that has been explicitly factored out, whereas the coefficients of the dipole operators retain dimensions of one inverse power of the mass. We will assume that the QCD θ term, arising at dimension-four in the SM, is removed by the Peccei-Quinn mechanism [76]. Moreover, we do not consider CP-odd four-fermion interactions (generated by tree-level $C_{1,2}$ exchange) as all couplings to first and second generation fermions are suppressed.

Elementary fermion EDMs and CEDMs originate first at the 3-loop level from the three loop, Barr-Zee type graphs shown in Fig. 7 [panel a]. This loop suppression arises from the need for a different phase in the Yukawa vertices in the fermion loop. Such a diagram requires mixing of $C_{1,2}$ mixing through Higgs portal interactions⁶. Naive dimensional analysis yields for the electron EDM

$$\begin{aligned} d_e & \simeq e\frac{\alpha_{EM}}{4\pi}\frac{\text{Im}(y_1y_2)}{(4\pi)^4}\frac{m_em_b^2}{m_C^4} \\ & \sim 5 \times 10^{-36} \text{Im}(y_1y_2)\left(\frac{\text{TeV}}{m_C}\right)^4 e \cdot \text{cm}. \end{aligned} \quad (50)$$

The scaling with m_C^{-4} is not surprising, since the C_1 - C_2 mixing an insertion of $\langle H^\dagger H \rangle$ associated with mixing in the scalar potential. For $m_C = 500$ GeV this gives $d_e \sim 10^{-34} \text{Im}(y_1y_2) e \cdot \text{cm}$, far below even the recent ACME bound $|d_e| < 8.7 \times 10^{-29} e \cdot \text{cm}$ [77], leaving the CP-odd phases unconstrained. Accordingly, we neglect all fermion (chromo-)EDMs.

The neutron EDM receives contributions from the quark EDM and chromo-EDM operators as well as the Weinberg three-gluon operator. For the light quarks, the (chromo-)EDMs will be enhanced compared to d_e by $m_q/m_e \sim 10$, where m_q is the light quark mass. The resulting contribution will, nevertheless, be far too small to be experimentally relevant.

The neutron EDM, d_N , and the isoscalar P and T odd pion-nucleon coupling \bar{g}_π^0 are both sensitive to the Weinberg operator. Following Ref. [72] one can relate both d_N and \bar{g}_π^0 to the Wilson coefficient of the Weinberg operator

$$d_N = \frac{v^2}{m_C^2} \text{Im}[C_W] \beta_{\tilde{G}} \quad (51)$$

$$\bar{g}_\pi^0 = \frac{v^2}{m_C^2} \text{Im}[C_W] \gamma_{\tilde{G}} \quad (52)$$

where

$$\beta_{\tilde{G}} = [2 - 40] \times 10^{-7} e \cdot fm, \quad \gamma_{\tilde{G}} = [1 - 10] \times 10^{-6}. \quad (53)$$

Based on the diagram in Fig. 7 [panel b], we estimate C_W at the weak scale, obtaining

$$C_W = \frac{g_s^2}{(4\pi)^4} \text{Im}(y_1y_2) f\left(\frac{m_C^2}{m_b^2}\right). \quad (54)$$

Here f is a 2-loop function which we identify with that calculated in Ref. [78]. We emphasize that, since the internal scalar lines themselves have $SU(3)_C$ charge and can also emit gluons, the true loop function inevitably differs from that of Ref. [78]. However, we expect such contributions to be suppressed relative to Eqs. (51) and (52) due to their explicit momentum dependence so we persist for now with the above estimate.

Following Ref. [79–81], the running of the Weinberg operator coefficient from the weak scale to the hadronic scale is given by

$$C_W(M_{\text{QCD}}) = \left(\frac{\alpha_s(M_W)}{\alpha_s(M_{\text{QCD}})}\right)^{\gamma_G/(2\beta_0)} C_W(M_W). \quad (55)$$

with anomalous dimension $\gamma_G = N_c + 2n_f + \beta_0$, $\beta_0 = 11 - 2/3n_f$, and $n_f \equiv$ the number of active quark flavors. As heavy quark flavors are integrated out at their respective masses, threshold effects arise [82], inducing a shift in C_W proportional to the corresponding CEDM. In particular, such a shift occurs at the b -quark mass threshold and can lead to significant effects if \tilde{d}_b can be generated at the 1-loop level. However, as $C_{1,2}$ couple only to b_R , generation of \tilde{d}_b still arises from the Bar-Zee graphs in Fig. 7 [panel a], rendering the resulting shift completely negligible.

The resulting estimate for the neutron EDM and \bar{g}_π^0 are then

$$\begin{aligned} d_N & \approx [3 - 60] \times 10^{-25} \frac{v^2}{m_C^2} \text{Im}(y_1y_2) f\left(\frac{m_C^2}{m_b^2}\right) e \cdot \text{cm} \\ \bar{g}_\pi^0 & \approx [1.5 - 15] \times 10^{-11} \frac{v^2}{m_C^2} \text{Im}(y_1y_2) f\left(\frac{m_C^2}{m_b^2}\right) \end{aligned} \quad (56)$$

which, for $m_C = 500$ GeV, gives $d_N \simeq 10^{-28} \text{Im}(y_1y_2)$. The current upper limit on the neutron EDM is set at the 90% C.L. as $|d_n| < [2.9 - 3.0] \times 10^{-26} e \cdot \text{cm}$ [83, 84], implying that next-generation neutron EDM experiments

⁶ Note that inclusion of unsuppressed first and second generation leptoquark interactions one give rise to one-loop elementary fermion (chromo-) EDMs

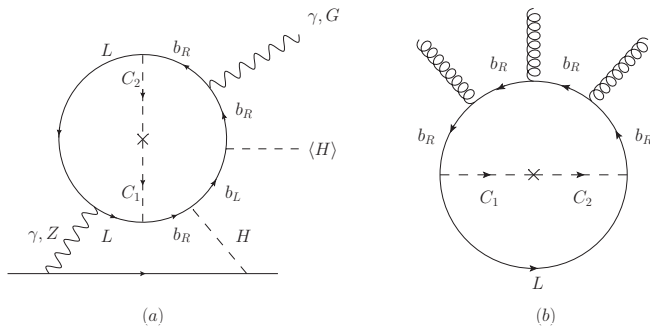


FIG. 7: Panel (a): Fermion EDMs and chromo-EDMs arise at the 3-loop level, precluding any resulting constructive bounds on the parameter space from these sources. Panel (b): The neutron EDM is sensitive to CP violation in CoBBG through the Weinberg operator. Next generation experiments searching for neutron EDMs require an improvement of roughly $\mathcal{O}(10^3)$ in order to test the CoBBG scenario.

require improvements of $\mathcal{O}(10^2-10^3)$ to directly probe the CP violation responsible for baryon production during the CoB phase transition. The current upper limit on the isoscalar coupling is $|\bar{g}_\pi^0| < 3.8 \times 10^{-12}$ [74] and we similarly find we are at least two orders of magnitude below this bound for a leptoquark mass of 500 GeV. So contributions to EDMs are indeed constrained within our model. However, we make the following two caveats to our analysis

- Under our current assumption of a CP-conserving potential, the operators responsible for $C_{1,2}$ mixing do not themselves contribute a phase and thus precision measurements of EDMs directly constrain the phase responsible for baryon production during the CoB transition. If this assumption is relaxed, the connection between the CP violation responsible for baryon production and that appearing in EDMs becomes less clear.
- The values of $\beta_{\bar{G}}$ and $\gamma_{\bar{G}}$ are quite uncertain and span an order of magnitude.

We leave a thorough calculation of each EDM as well as consideration of these issues to a future project.

VI. CONCLUSIONS

EWBG links the generation of the cosmic baryon asymmetry to electroweak symmetry breaking in the

early universe. In contrast to other theoretically well-motivated scenarios, it is one of the most testable, since it involves new weak scale physics. Not surprisingly, null results for permanent EDMs as well as new particle searches at the LHC tightly constrain EWBG models.

In this work we have relaxed the assumption that today's symmetries have always been symmetries of nature throughout our cosmic history [16–26]. We specifically examine the possibility that $SU(3)_C$ was broken for a period and then subsequently restored [25]. This framework of CoB represents a new EWBG paradigm. We have presented an implementation of this framework that successfully reproduces the BAU without significant fine-tuning while evading present experimental constraints. The framework is still testable because the leptoquark couplings cannot be arbitrarily small, nor can their masses be arbitrarily heavy.

In CoB, the BAU is generated during an intermediate color breaking phase transition. We consider the case where color-breaking fields couple to SM fermions so as to avoid stable colored relics. Furthermore, in our implementation the interaction between the color breaking fields and the standard model fermions conserve $B-L$. As such, the spontaneous breaking and restoration of $SU(3)_C$ is associated with spontaneous breaking and restoration of $B-L$. However, during the color-breaking transition a $B+L$ asymmetry is generated through the electroweak mechanism which persists even when $B-L$ is restored. The contribution from the spontaneous violation of $B-L$ is negligible as any such contribution is quickly relaxed away from the bubble wall.

We conclude by noting that our particular implementation of CoB was a proof of concept. There are other possible implementations of CoB and to truly test the viability of any particular model one would need to simultaneously examine the phase transition and the transport dynamics. We leave such an examination to future work.

Acknowledgments

We thank Lorenzo Sorbo for helpful discussions. GW would like to acknowledge that his contribution to this work was partly funded by both the American Australian Association via the Keith Murdoch fellowship as well the Australian Postgraduate Award (APA). MJRM and PW were supported in part under U.S. Department of Energy contract de-sc0011095.

[1] Planck, P. A. R. Ade *et al.*, *Astron. Astrophys.* **571**, A16 (2014), 1303.5076.
 [2] A. D. Sakharov, *Pisma Zh. Eksp. Teor. Fiz.* **5**, 32 (1967), [*Usp. Fiz. Nauk*161,61(1991)].

[3] M. B. Gavela, P. Hernandez, J. Orloff, and O. Pene, *Mod. Phys. Lett.* **A9**, 795 (1994), hep-ph/9312215.
 [4] P. Huet and E. Sather, *Phys. Rev.* **D51**, 379 (1995), hep-ph/9404302.

- [5] M. B. Gavela, P. Hernandez, J. Orloff, O. Pene, and C. Quimbay, Nucl. Phys. **B430**, 382 (1994), hep-ph/9406289.
- [6] M. Gurtler, E.-M. Ilgenfritz, and A. Schiller, Phys. Rev. **D56**, 3888 (1997), hep-lat/9704013.
- [7] M. Laine and K. Rummukainen, Nucl. Phys. Proc. Suppl. **73**, 180 (1999), hep-lat/9809045.
- [8] F. Csikor, Z. Fodor, and J. Heitger, Phys. Rev. Lett. **82**, 21 (1999), hep-ph/9809291.
- [9] Y. Aoki, F. Csikor, Z. Fodor, and A. Ukawa, Phys. Rev. **D60**, 013001 (1999), hep-lat/9901021.
- [10] M. Trodden, Rev. Mod. Phys. **71**, 1463 (1999), hep-ph/9803479.
- [11] D. E. Morrissey and M. J. Ramsey-Musolf, New J. Phys. **14**, 125003 (2012), 1206.2942.
- [12] G. A. White, *A Pedagogical Introduction to Electroweak Baryogenesis* IOP Concise Physics (Morgan and Claypool, 2016).
- [13] D. Curtin, P. Jaiswal, and P. Meade, JHEP **08**, 005 (2012), 1203.2932.
- [14] A. Katz, M. Perelstein, M. J. Ramsey-Musolf, and P. Winslow, Phys. Rev. **D92**, 095019 (2015), 1509.02934.
- [15] S. Liebler, S. Profumo, and T. Stefaniak, JHEP **04**, 143 (2016), 1512.09172.
- [16] S. Weinberg, Phys. Rev. **D9**, 3357 (1974).
- [17] R. N. Mohapatra and G. Senjanovic, Phys. Rev. Lett. **42**, 1651 (1979).
- [18] R. N. Mohapatra and G. Senjanovic, Phys. Rev. **D20**, 3390 (1979).
- [19] P. Langacker and S.-Y. Pi, Phys. Rev. Lett. **45**, 1 (1980).
- [20] A. Hammerschmitt, J. Kripfganz, and M. G. Schmidt, Z. Phys. **C64**, 105 (1994), hep-ph/9404272.
- [21] G. R. Dvali, A. Melfo, and G. Senjanovic, Phys. Rev. Lett. **75**, 4559 (1995), hep-ph/9507230.
- [22] G. R. Dvali, A. Melfo, and G. Senjanovic, Phys. Rev. **D54**, 7857 (1996), hep-ph/9601376.
- [23] J. M. Cline, G. D. Moore, and G. Servant, Phys. Rev. **D60**, 105035 (1999), hep-ph/9902220.
- [24] H. H. Patel and M. J. Ramsey-Musolf, Phys. Rev. **D88**, 035013 (2013), 1212.5652.
- [25] H. H. Patel, M. J. Ramsey-Musolf, and M. B. Wise, Phys. Rev. **D88**, 015003 (2013), 1303.1140.
- [26] N. Blinov, J. Kozaczuk, D. E. Morrissey, and C. Tamarit, Phys. Rev. **D92**, 035012 (2015), 1504.05195.
- [27] F. Jona and G. Shirane, *Ferroelectric Crystals* (Oxford: Pergamon, 1962).
- [28] Particle Data Group, K. A. Olive *et al.*, Chin. Phys. **C38**, 090001 (2014).
- [29] J. M. Arnold, B. Fornal, and M. B. Wise, Phys. Rev. **D88**, 035009 (2013), 1304.6119.
- [30] H. Murayama and T. Yanagida, Mod. Phys. Lett. **A7**, 147 (1992).
- [31] ATLAS, G. Aad *et al.*, Eur. Phys. J. **C76**, 5 (2016), 1508.04735.
- [32] A. Riotto, Phys. Rev. **D58**, 095009 (1998), hep-ph/9803357.
- [33] M. Carena, M. Quiros, M. Seco, and C. E. M. Wagner, Nucl. Phys. **B650**, 24 (2003), hep-ph/0208043.
- [34] T. Konstandin, T. Prokopec, M. G. Schmidt, and M. Seco, Nucl. Phys. **B738**, 1 (2006), hep-ph/0505103.
- [35] C. Lee, V. Cirigliano, and M. J. Ramsey-Musolf, Phys. Rev. **D71**, 075010 (2005), hep-ph/0412354.
- [36] J. S. Schwinger, J. Math. Phys. **2**, 407 (1961).
- [37] K. T. Mahanthappa, Phys. Rev. **126**, 329 (1962).
- [38] P. M. Bakshi and K. T. Mahanthappa, Journal of Mathematical Physics **4**, 1 (1963).
- [39] P. M. Bakshi and K. T. Mahanthappa, Journal of Mathematical Physics **4**, 12 (1963).
- [40] L. V. Keldysh, Zh. Eksp. Teor. Fiz. **47**, 1515 (1964), [Sov. Phys. JETP **20**, 1018 (1965)].
- [41] K. chao Chou, Z. bin Su, B. lin Hao, and L. Yu, Physics Reports **118**, 1 (1985).
- [42] V. Cirigliano, C. Lee, M. J. Ramsey-Musolf, and S. Tulin, Phys. Rev. **D81**, 103503 (2010), 0912.3523.
- [43] V. Cirigliano, C. Lee, and S. Tulin, Phys. Rev. **D84**, 056006 (2011), 1106.0747.
- [44] T. Liu, M. J. Ramsey-Musolf, and J. Shu, Phys. Rev. Lett. **108**, 221301 (2012), 1109.4145.
- [45] D. Curtin, P. Meade, and H. Ramani, (2016), 1612.00466.
- [46] S. Inoue, G. Ovanessian, and M. J. Ramsey-Musolf, Phys. Rev. **D93**, 015013 (2016), 1508.05404.
- [47] A. G. Cohen, D. B. Kaplan, and A. E. Nelson, Phys. Lett. **B336**, 41 (1994), hep-ph/9406345.
- [48] D. Bodeker, G. D. Moore, and K. Rummukainen, Phys. Rev. **D61**, 056003 (2000), hep-ph/9907545.
- [49] D. J. H. Chung, B. Garbrecht, M. J. Ramsey-Musolf, and S. Tulin, Phys. Rev. Lett. **102**, 061301 (2009), 0808.1144.
- [50] M. Joyce, T. Prokopec, and N. Turok, Phys. Rev. **D53**, 2930 (1996), hep-ph/9410281.
- [51] M. Joyce, T. Prokopec, and N. Turok, Phys. Rev. **D53**, 2958 (1996), hep-ph/9410282.
- [52] V. Cirigliano, M. J. Ramsey-Musolf, S. Tulin, and C. Lee, Phys. Rev. **D73**, 115009 (2006), hep-ph/0603058.
- [53] G. D. Moore and M. Tassler, JHEP **02**, 105 (2011), 1011.1167.
- [54] G. A. White, Phys. Rev. **D93**, 043504 (2016), 1510.03901.
- [55] P. John, Phys. Lett. **B452**, 221 (1999), hep-ph/9810499.
- [56] S. Akula, C. Balazs, and G. A. White, Eur. Phys. J. **C76**, 681 (2016), 1608.00008.
- [57] C. Balazs, G. White, and J. Yue, JHEP **03**, 030 (2017), 1612.01270.
- [58] S. Akula, C. Balazs, L. Dunn, and G. White, (2017), 1706.09898.
- [59] J. M. Moreno, M. Quiros, and M. Seco, Nucl. Phys. **B526**, 489 (1998), hep-ph/9801272.
- [60] J. Kozaczuk, S. Profumo, L. S. Haskins, and C. L. Wainwright, JHEP **01**, 144 (2015), 1407.4134.
- [61] CMS, A. M. Sirunyan *et al.*, JHEP **07**, 121 (2017), 1703.03995.
- [62] J. F. Gunion, H. E. Haber, G. L. Kane, and S. Dawson, Front. Phys. **80**, 1 (2000).
- [63] CMS, C. Collaboration, (2017).
- [64] ATLAS, T. A. collaboration, (2017).
- [65] ATLAS, M. Aaboud *et al.*, (2017), 1708.03299.
- [66] ATLAS, CMS, G. Aad *et al.*, JHEP **08**, 045 (2016), 1606.02266.
- [67] CERN Report No. ATL-PHYS-PUB-2013-014, 2013 (unpublished).
- [68] CMS, Projected Performance of an Upgraded CMS Detector at the LHC and HL-LHC: Contribution to the Snowmass Process, in *Community Summer Study 2013: Snowmass on the Mississippi (CSS2013) Minneapolis, MN, USA, July 29-August 6, 2013*, 2013, 1307.7135.
- [69] The fifth Annual Large Hadron Collider Physics conference, 2017, Higgs boson measurements at LHC after upgrade.
- [70] F. De Almeida Dias, CERN Report No. ATL-PHYS-

- PROC-2015-081, 2015 (unpublished).
- [71] M. Pospelov and A. Ritz, *Annals Phys.* **318**, 119 (2005), hep-ph/0504231.
- [72] J. Engel, M. J. Ramsey-Musolf, and U. van Kolck, *Prog. Part. Nucl. Phys.* **71**, 21 (2013), 1303.2371.
- [73] T. Chupp and M. Ramsey-Musolf, *Phys. Rev. C* **91**, 3 (2015), 1407.1064v1.
- [74] T. Chupp, P. Fierlinger, M. Ramsey-Musolf, and J. Singh, unpublished, To appear, 2017.
- [75] S. Weinberg, *Phys. Rev. Lett.* **63**, 2333 (1989).
- [76] R. D. Peccei and H. R. Quinn, *Phys. Rev. Lett.* **38**, 1440 (1977).
- [77] ACME, J. Baron *et al.*, *Science* **343**, 269 (2014), 1310.7534.
- [78] D. A. Dicus, *Phys. Rev. D* **41**, 999 (1990).
- [79] S. M. G. Degrossi, E. Franco and L. Silvestrini, *JHEP* **0511**, 044 (2005).
- [80] J. Hisano, K. Tsumura, and M. J. S. Yang, *Phys. Lett.* **B713**, 473 (2012), 1205.2212.
- [81] W. Dekens and J. de Vries, *JHEP* **05**, 149 (2013), 1303.3156.
- [82] C. S. L. E. Braaten and T. C. Yuan, *Phys. Rev. Lett.* **64**, 1709 (1990).
- [83] C. A. Baker *et al.*, *Phys. Rev. Lett.* **97**, 131801 (2006).
- [84] J. M. Pendlebury *et al.*, *Phys. Rev.* **D92**, 092003 (2015), 1509.04411.

Appendix

Here, we provide a table of charge values associated with all symmetries in the symmetric, CoB, and electroweak phases for all particle species.

State	Q_{T^3}	Q_{T^8}	Q_{τ^3}	Q_Y	$Q_{X_1} = Q_{T^8} - \frac{2}{\sqrt{3}} Q_{\tau^3}$	$Q_{X_2} = Q_{\tau^3} + 3Q_Y$
$\{u_{1L}, u_{2L}, u_{3L}\}$	$\{\frac{1}{2}, -\frac{1}{2}, 0\}$	$\{\frac{1}{2\sqrt{3}}, \frac{1}{2\sqrt{3}}, -\frac{1}{\sqrt{3}}\}$	$\frac{1}{2}$	$\frac{1}{6}$	$\{-\frac{1}{2\sqrt{3}}, -\frac{1}{2\sqrt{3}}, -\frac{2}{\sqrt{3}}\}$	1
$\{d_{1L}, d_{2L}, d_{3L}\}$	$\{\frac{1}{2}, -\frac{1}{2}, 0\}$	$\{\frac{1}{2\sqrt{3}}, \frac{1}{2\sqrt{3}}, -\frac{1}{\sqrt{3}}\}$	$-\frac{1}{2}$	$\frac{1}{6}$	$\{\frac{\sqrt{3}}{2}, -\frac{\sqrt{3}}{2}, 0\}$	0
$\{u_{1R}, u_{2R}, u_{3R}\}$	$\{\frac{1}{2}, -\frac{1}{2}, 0\}$	$\{\frac{1}{2\sqrt{3}}, \frac{1}{2\sqrt{3}}, -\frac{1}{\sqrt{3}}\}$	0	$\frac{2}{3}$	$\{\frac{1}{2\sqrt{3}}, \frac{1}{2\sqrt{3}}, -\frac{1}{\sqrt{3}}\}$	2
$\{d_{1R}, d_{2R}, d_{3R}\}$	$\{\frac{1}{2}, -\frac{1}{2}, 0\}$	$\{\frac{1}{2\sqrt{3}}, \frac{1}{2\sqrt{3}}, -\frac{1}{\sqrt{3}}\}$	0	$-\frac{1}{3}$	$\{\frac{1}{2\sqrt{3}}, \frac{1}{2\sqrt{3}}, -\frac{1}{\sqrt{3}}\}$	-1
e_L	0	0	$-\frac{1}{2}$	$-\frac{1}{2}$	$\frac{1}{\sqrt{3}}$	-2
ν_L	0	0	$\frac{1}{2}$	$-\frac{1}{2}$	$-\frac{1}{\sqrt{3}}$	-1
H^+	0	0	$\frac{1}{2}$	$\frac{1}{2}$	$-\frac{1}{\sqrt{3}}$	2
H^0	0	0	$\frac{1}{2}$	$\frac{1}{2}$	$\frac{1}{\sqrt{3}}$	1
W_μ^\pm	0	0	± 1	0	$\mp \frac{2}{\sqrt{3}}$	± 1
$\{\chi_1^{2/3}, \chi_2^{2/3}, \chi_3^{2/3}\}$	$\{\frac{1}{2}, -\frac{1}{2}, 0\}$	$\{\frac{1}{2\sqrt{3}}, \frac{1}{2\sqrt{3}}, -\frac{1}{\sqrt{3}}\}$	$\frac{1}{2}$	$\frac{1}{6}$	$\{-\frac{1}{2\sqrt{3}}, -\frac{1}{2\sqrt{3}}, -\frac{2}{\sqrt{3}}\}$	1
$\{\chi_1^{-1/3}, \chi_2^{-1/3}, \chi_3^{-1/3}\}$	$\{\frac{1}{2}, -\frac{1}{2}, 0\}$	$\{\frac{1}{2\sqrt{3}}, \frac{1}{2\sqrt{3}}, -\frac{1}{\sqrt{3}}\}$	$-\frac{1}{2}$	$\frac{1}{6}$	$\{\frac{\sqrt{3}}{2}, -\frac{\sqrt{3}}{2}, 0\}$	0
$\{G_\mu^{\pm,12}, G_\mu^{\pm,45}, G_\mu^{\pm,67}\}$	$\{\pm 1, \pm 1/2, \mp 1/2\}$	$\{0, \pm \frac{\sqrt{3}}{2}, \pm \frac{\sqrt{3}}{2}\}$	0	0	$\{0, \pm \frac{\sqrt{3}}{2}, \pm \frac{\sqrt{3}}{2}\}$	0

TABLE I: Table of charges for all species in the plasma. Singular values for a given charge imply that all colors have the same charge.